

# The Eye Organizes Neural Crest Cell Migration

Tobias Langenberg,<sup>1</sup> Alon Kahana,<sup>2†</sup> Joseph A. Wszalek,<sup>1</sup> and Mary C. Halloran<sup>1\*</sup>

In the anterior vertebrate head, a population of neural crest cells (NCCs) migrates to the periocular mesenchyme and makes critical contributions to the developing eye and orbit. Improper migration and differentiation of these NCCs have been implicated in human diseases such as congenital glaucoma and anterior segment dysgenesis syndromes. The mechanisms by which these cells migrate to their target tissues within and around the eye are not well understood. We present a fate map of zebrafish diencephalic and mesencephalic NCC contributions to the eye and orbit. The fate map closely resembles that in chick and mice, demonstrating evolutionary conservation. To gain insight into the mechanisms of anterior NCC guidance, we used the eyeless mutant *chokh/rx3*. We show that, in *chokh* mutants, dorsal anterior NCC migration is severely disorganized. Time-lapse analysis shows that NCCs have significantly reduced migration rates and directionality in *chokh* mutants. *Developmental Dynamics* 237:1645–1652, 2008.

© 2008 Wiley-Liss, Inc.

**Key words:** zebrafish; neural crest; periocular mesenchyme; eye; anterior segment; orbit

Accepted 14 April 2008

## INTRODUCTION

Early in vertebrate development, the emerging eye is surrounded by mesenchymal cells derived from both lateral plate mesoderm and neural crest (NC), which together form the periocular mesenchyme (POM). In the anterior segment of the eye, POM cells give rise to the corneal endothelium, keratocytes of the corneal stroma, the ciliary muscle, iris stroma, the sclera, choroidal pericytes, and the trabecular meshwork. In the periphery of the eye, these cells form orbital cartilages and bones, blood vessels, as well as connective tissue associated with the extraocular muscles (Noden, 1975, 1983; Le Lievre, 1978; Johnston et al., 1979; Meier, 1982; Couly and Le Douarin, 1987, 1990; Chan and Tam,

1988; Couly et al., 1992, 1993; Serbedzija et al., 1992; Osumi-Yamashita et al., 1994; Trainor et al., 1994; Trainor and Tam, 1995; Creuzet et al., 2005; Gage et al., 2005; Kanakubo et al., 2006). These neural crest-derived mesenchymal structures are critical to the normal function of the eye. For example, the mesenchyme-derived trabecular meshwork is needed to maintain physiologic intraocular pressure by controlling the outflow of aqueous humor. A malfunctioning trabecular meshwork will cause high pressure and glaucoma, a progressive degeneration of the optic nerve that is a leading cause of blindness worldwide. Several transcription factors are known to be required for differentiation of POM-derived structures (Cvekl

and Tamm, 2004). However, we still know very little about the mechanisms by which neural crest cells (NCCs) and mesenchymal cells migrate to form the POM and differentiate into the various structures within and surrounding the eye.

Owing to its optical clarity, genetics, and ease of manipulation, the zebrafish is an ideal model system to study mechanisms of NCC migration and differentiation. Fate mapping experiments have shown that the pharyngeal skeleton of zebrafish, like that of other vertebrate embryos, is largely derived from NCCs migrating from the hindbrain (Schilling and Kimmel, 1994). In contrast, the neurocranium is derived mostly from diencephalic and mesencephalic NCCs (Wada et

<sup>1</sup>Departments of Zoology and Anatomy, University of Wisconsin, Madison, Wisconsin

<sup>2</sup>Department of Ophthalmology and Visual Sciences, University of Wisconsin, Madison, Wisconsin

Grant sponsor: NIH; Grant number: NS042228; Grant sponsor: DFG; Grant number: LA2391/1-1.

<sup>†</sup>Dr. Kahana's present address is Department of Ophthalmology and Visual Sciences, University of Michigan, Kellogg Eye Center, 1000 Wall Street, Ann Arbor, MI 48109.

\*Correspondence to: Mary C. Halloran, Department of Zoology, 1117 W. Johnson Street, Madison, WI 53706.

E-mail: mchalloran@wisc.edu

DOI 10.1002/dvdy.21577

Published online 19 May 2008 in Wiley InterScience (www.interscience.wiley.com).

al., 2005; Eberhart et al., 2006). Fate mapping data from these studies demonstrated that NCCs from the diencephalon and mesencephalon take three different migratory routes: dorsal anterior to form the median ethmoid plate, medial to form the trabeculae and lateral ethmoid, and posterior to the eye into branchial arch 1 (BA1). To date, little is known about the development of the anterior eye segment and orbit in zebrafish. Although the anatomy of both orbital (Cubbage and Mabee, 1996) and anterior eye (Soules and Link, 2005) structures has been described, there are very few studies on the development of these elements. Moreover, it is currently unknown, in any species, how anterior NCCs split into different migration streams, find their way to target areas, and develop into very different structures within and around the eye.

In this study, we investigated the migration of NCCs to the eye and orbit. We labeled premigratory NCCs of the diencephalon and mesencephalon and mapped their position at 36 hours postfertilization (hpf). We show that there is a strong NC contribution to the dorsal orbit, eye, and frontonasal process. Similar to previous reports, we demonstrate that only mesencephalic NCCs contribute to BA1 and that NCCs migrate along three different routes (Wada et al., 2005). To investigate the role of the developing eye in NCC migration, we analyzed NCCs in the eyeless mutant *chokh/rx3*. Our results demonstrate that the eye is necessary for the migration of the dorsal anterior NC subpopulation and dispensable for the medial and BA1 populations. As a result, *chokh* embryos lack all of the dorsal orbit and most of the ethmoid plate, but display an otherwise normal neurocranium and pharyngeal cartilages.

## RESULTS

To analyze the migration pattern of anterior NCCs contributing to the POM in zebrafish, we labeled wild-type (WT) embryos between the 6-somite stage (ss) and 36 hpf for expression of *crestin*, a specific pan-NCC marker (Luo et al., 2001). At the 6–8 ss, a large population of NCCs is located at the dorsal posterior end of the

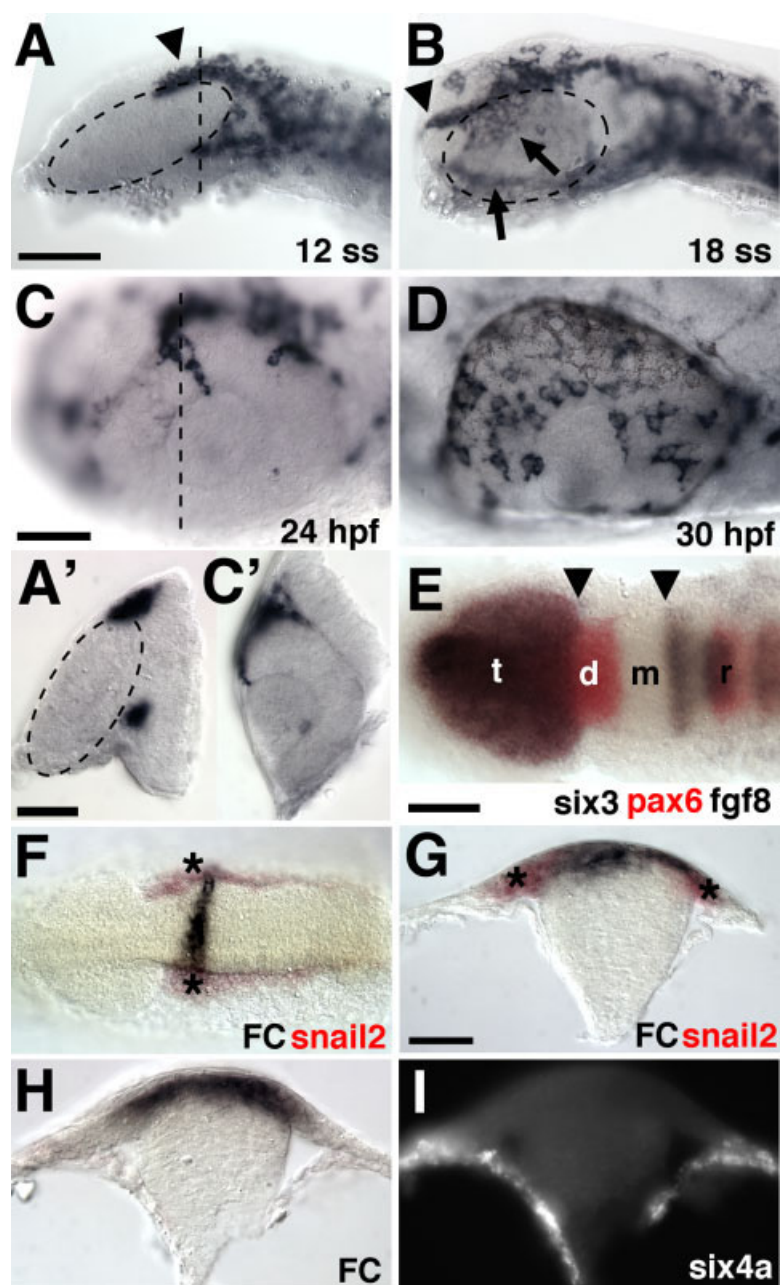


**Fig. 1.** Anterior neural crest localization and uncaging method. **A–D:** In situ hybridization for *crestin* at the indicated stages. Anterior is to the left, dorsal is up. **A'** and **C'** are cross-sections of **A** and **C**, respectively, sectioned at the dotted lines. Arrowheads point to the dorsal anterior stream of neural crest cells (NCCs), arrows to the medial and ventral populations. The hatched oval outlines the eye. **E:** Double in situ hybridization for the indicated genes. Dorsal view, anterior to the left. Arrowheads mark the boundaries of the regions uncaged for fate mapping. t, telencephalon; d, diencephalon; m, mesencephalon; r, rhombencephalon. **F–I:** Controls showing that NCCs and not lateral plate mesoderm were uncaged. Uncaged fluorescein (FC) stained black. **F,G:** Dorsal view (**F**) and (**G**) cross-section (**G**) showing uncaged fluorescein (black) and *snail2* expressing NCCs (red, asterisks). **I:** Fluorescent in situ hybridization for *six4a*, which is masked by the bright background in **H**. **G–I** are cross-sections. Scale bars = 100  $\mu$ m in **A,B**, 50  $\mu$ m in **C,D**, 25  $\mu$ m in **A',C'**, 100  $\mu$ m in **E,F**, 50  $\mu$ m in **G–I**.

developing eye (Thisse et al., 1995; Dutton et al., 2001; Luo et al., 2001). Between the 10 and 12 ss, this group of cells appears to move anteriorly with respect to the eye (Thisse et al.,

1995; Dutton et al., 2001; Fig. 1A, arrowhead, **A'**). Over the next 3 hr of development, *crestin*-positive cells are seen progressively closer to the anterior tip of the embryo (Fig. 1B, arrow-

head), as well as ventral and medial to the eye (Fig. 1B, arrows). NCCs can be detected for the first time on the surface of the eye at 23–24 hpf (Fig. 1C). They are located between the future corneal epithelium and the neural retina (Fig. 1C'). Within the next several hours of development, the entire surface of the eye is populated by *crestin*-positive cells (Fig. 1D).

To determine the origin of NCCs contributing specifically to the eye and orbit, we carried out fate mapping experiments. We labeled groups of premigratory NCCs in the diencephalon and mesencephalon by photoconversion of caged fluorescein. The brain regions were targeted by comparison with age-matched embryos labeled by *in situ* hybridization for *six3*, whose expression boundary demarks the telencephalic–diencephalic border, *pax6*, which marks the diencephalic–mesencephalic boundary, and *fgf8*, which labels the mesencephalic–rhombencephalic border (Fig. 1E). Because both mesodermal cells and NCCs contribute to the eye and orbit (Johnston et al., 1979; Noden, 1986a,b; Couly et al., 1992, 1993; Trainor et al., 1994; Trainor and Tam, 1995; Jiang et al., 2002; Gage et al., 2005), and these cells are adjacent to each other at the 6–8 ss, we needed to devise an uncaging approach that would specifically label neuroepithelial cells and NCCs but not mesodermal cells. We injected embryos with caged fluorescein at the one-cell stage. At the 6–8 ss, embryos were mounted laterally and a small region of NCCs and neuroepithelial cells was uncaged by exposing the dorsal edge of the neural keel to a brief ultraviolet pulse. We fixed embryos immediately after uncaging and labeled them with an antibody to fluorescein and with *in situ* hybridization for either *snail2*, which labels NCCs at this stage, or *six4a*, which labels lateral plate mesoderm (Seo et al., 1998). This labeling shows that the uncaged area lies within the expression domain of *snail2* (Fig. 1F,G, asterisks) and outside that of *six4a* (Fig. 1H,I). We conclude that our method only marks NCCs and neuroepithelial, but not mesodermal cells.

For the fate mapping experiments, we used this uncaging method and allowed embryos to develop to 36 hpf, when they were fixed and labeled for

uncaged fluorescein. We found that NCCs from specific anterior–posterior locations contribute to specific orbital regions and other neurocranial structures (Fig. 2). NCCs from the diencephalon contribute to the anterior dorsal and ventral orbit and the eye, and are also found surrounding the olfactory placodes (Fig. 2A–C,C'). NCCs stemming from the anterior midbrain colonize the eye, with a tendency toward the posterior half, as well as the posterior dorsal orbit (Fig. 2D–F,F'). The posterior midbrain contributes relatively few NCCs to the eye and orbit, and also makes a contribution to BA1 (Fig. 2G–I, arrowhead in I). NCCs stemming from the midbrain–hindbrain boundary migrate into BA1. The results of all the fate mapping experiments ( $n = 60$  embryos) are summarized in Figure 3. Our data are in good agreement with previous fate mapping studies (Wada et al., 2005; Eberhart et al., 2006) and also demonstrate evolutionary conservation between zebrafish, chicken, and mice in the anterior cephalic NCC contribution to the eye.

To gain insight into the mechanism guiding NCC migration to the eye, we asked whether the eye is required for proper NCC migration. To this end, we made use of the eyeless zebrafish mutant *chokh/rx3*. *chokh* embryos carry a mutation in the transcription factor *rx3* (retina homeobox 3), which is normally expressed in the ventral medial forebrain and optic vesicles (Chuang et al., 1999). Loss of *rx3* function leads to the transformation of retinal precursor cells to a telencephalic fate, but does not affect patterning of the nervous system (Loosli et al., 2003; Kennedy et al., 2004; Rojas-Munoz et al., 2005; Stigloher et al., 2006). Of the known mutants with eye loss, *chokh* is the most specific, in that the defect is restricted to eye loss. We first examined the expression patterns of several NCC marker genes in *chokh* mutant embryos during somitogenesis stages (Fig. 4). Based on *snail2* expression, which labels all NCCs during NC induction and early migration (Thisse et al., 1995), we did not observe any difference in NCC induction between mutant embryos and wild-type siblings at the 8 ss (Fig. 4A,B). However, shortly after the onset of migration (14 ss), *chokh* embryos dis-

played a prominent reduction in cells expressing *sox10*, *crestin*, and *snail2* in the dorsal migratory stream (Fig. 4C,C',D,D', and data not shown). In contrast, the medial stream appeared to be less affected. This phenotype was still observed during late somitogenesis stages, when, at most, a few isolated cells expressing NCC markers were found in the dorsal anterior stream, while NCCs could be detected medial to the remnant of the lens in *chokh* embryos (Fig. 4E,E',F,F').

The loss of NCC marker expression could be due to either a failure of NCCs to migrate or a loss of NC character and accompanying down-regulation of NC marker genes within these cells. To specifically examine NCC migration, we performed time-lapse imaging of NCCs in *chokh* embryos. We crossed the *chokh* mutant line into the *Tg(sox10:gfp)* transgenic line, in which most NCCs express green fluorescent protein (GFP) at early stages under the control of a *sox10* promoter fragment (Wada et al., 2005). We reasoned that the GFP protein would be sufficiently stable to be present in migrating NCCs even after a potential loss of NCC character.

We first imaged embryos at lower magnification over extended time periods (approximately 10–18 ss) to determine the overall pattern of anterior NCC migration. In *Tg(sox10:gfp)* embryos, NCCs form an arch over the dorsal edge of the eye vesicle by migrating both anteriorly and posteriorly around the eye (Fig. 5A, arrowheads). Simultaneously, a second group of cells detaches from this arch-like cluster and migrates medially to the eye in a ventral–anterior direction (Fig. 5A, arrows). NCCs stream around the olfactory placodes in later stages (Figs. 5A, 6 hr panel, and Fig. 2C,C'). In contrast, in *chokh* embryos, GFP-positive NCCs green fluorescent protein (GFP)-positive NCCs in the dorsal migratory stream do not migrate anteriorly (Fig. 5B, arrowheads). Instead, these cells remain in a posterior location, appear disorganized and often spread out over a larger dorsal–ventral area than in WT embryos (Fig. 5B, asterisk). We never observed an arch-like organization of NCCs in *chokh* embryos.

To further characterize the defects in migratory behavior, we imaged

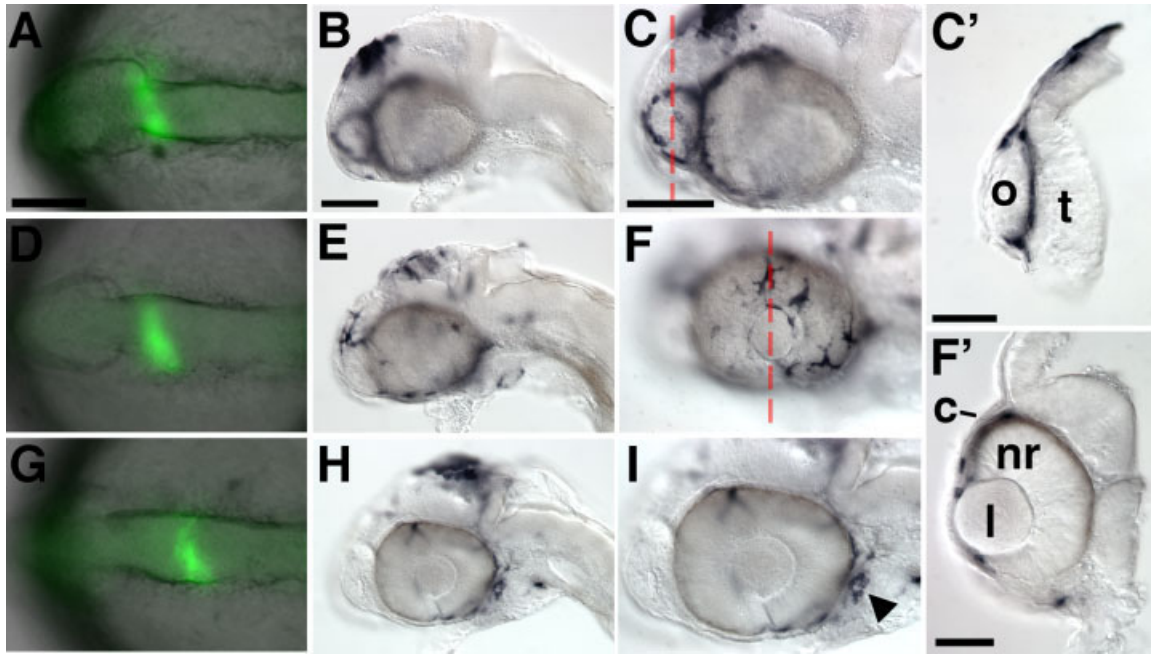


**Fig. 2.** Fate mapping of diencephalic and mesencephalic neural crest cells (NCCs). **A,D,G:** Live embryos at 6- to 8-somite stage (ss), immediately after uncaging, showing overlay of brightfield and uncaged fluorescein (green). Fluorescent signal is enhanced to stand out against background. Dorsal views, anterior to the left. **B,C,E,F,H,I:** Embryos at 36 hours postfertilization (hpf), labeled with anti-fluorescein antibody. Except for C' and F' all images are lateral views, anterior to the left. **A-C,C':** Diencephalic label. C': Cross-section through the telencephalon and olfactory placode (o) of the embryo in C. **D-F:** Mesencephalic label. F': Cross-section through one eye of the embryo in F. Fluorescein positive NCCs are located between the corneal epithelium (c) and the neural retina (nr). **G-I:** Posterior mesencephalic label. NCCs in BA1 are marked by the arrowhead. c, corneal epithelium; l, lens; nr, neural retina; o, olfactory placode; t, telencephalon. Scale bars = 100  $\mu$ m in A,D,G, 100  $\mu$ m in B,E,H, 50  $\mu$ m in C,F,I.

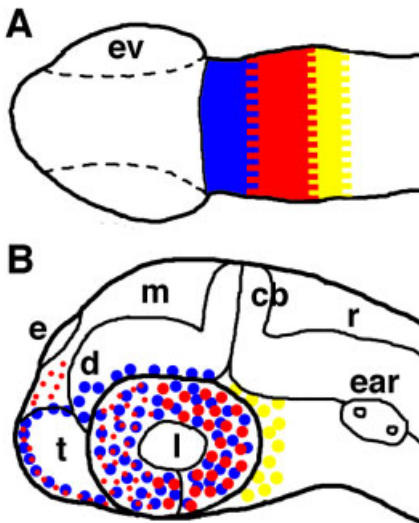


**Fig. 3.** Schematic summary of the fate mapping results derived from 60 embryos. **A:** Dorsal schematic view at the 6- to 8-somite stage (ss), anterior to the left. **B:** Lateral schematic view at 36 hpf, anterior to the left. Large dots indicate major, small dots minor contribution. Hatched areas illustrate limited resolution of the fate map. cb, cerebellum; d, diencephalon; e, epiphysis; ev, eye vesicle; l, lens; m, midbrain; r, rhombencephalon (hindbrain); t, telencephalon.

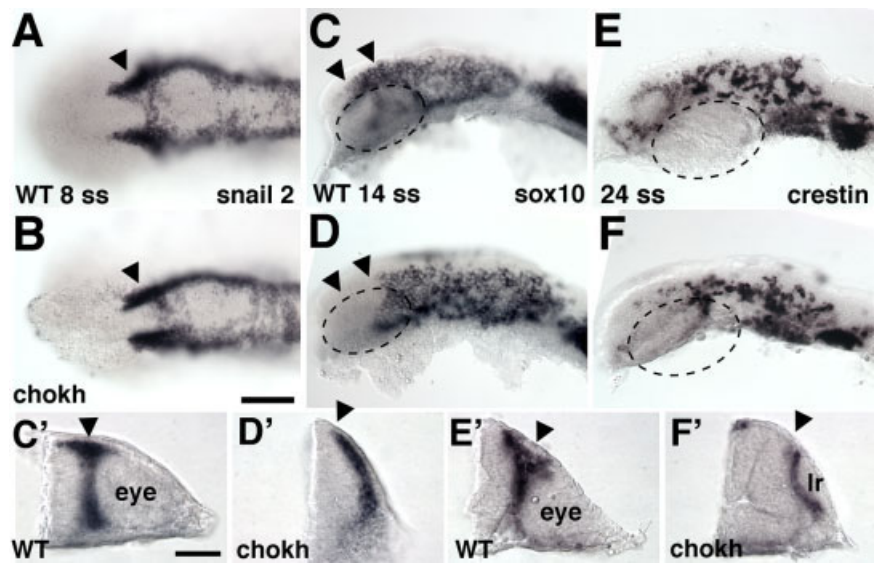


**Fig. 4.** Neural crest cells (NCCs) in *chokh* embryos. **A-F:** Wild-type (WT) and *chokh* mutant embryos labeled with in situ hybridization for NC markers at the indicated stages. Arrowheads mark normal (A-C,C',E') and missing (D,D',F') NCC populations. The hatched circle marks the eye in WT embryos (C,E) and the approximate position where the eye would normally have developed in *chokh* embryos (D,F). A, B are dorsal, C-F lateral views, anterior to the left. **C'-F':** Cross-sections through the eye vesicle in WT and the respective region in *chokh* embryos. Scale bar = 100  $\mu$ m in A-F, 50  $\mu$ m in C'-F'. lr, lens remnant.

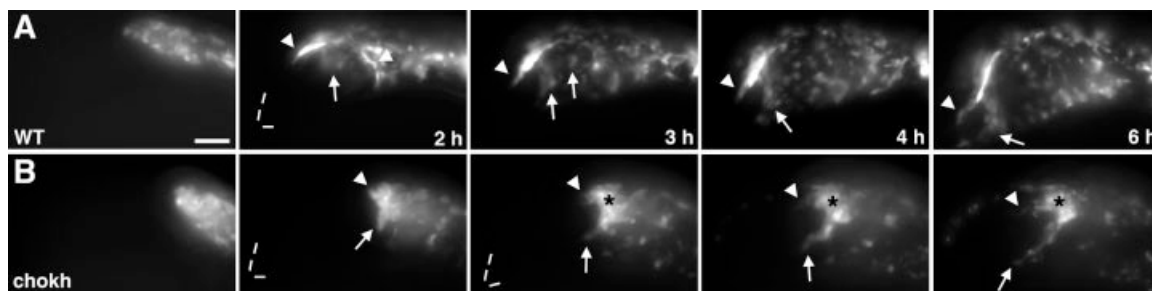


**Fig. 5.** Anterior neural crest cells (NCCs) have defective migration in *chokh*. **A,B:** Stills from time-lapse movies of a wild-type (WT, A) and a *chokh* mutant (B) embryo in the *Tg(sox10:gfp)* background. Images are a selection of maximum projections of stacks acquired every 5 min in a time-lapse. All images are lateral views with anterior to the left and dorsal up. In some panels, the tip of the embryo is marked by hatched lines. Arrowheads point to the dorsal anterior population of NCCs, arrows to the medial. The asterisk marks the mass of nonmigrating NCCs in *chokh* embryos. Scale bar = 100  $\mu\text{m}$ .

NCCs in the dorsal migratory population at higher magnification and shorter time intervals. We focused on the initial stages of migration, before NCCs contact the eye. Because we did not image past the 12 ss, NCCs in WT embryos reached the dorsal surface of the eye only toward the very end of the imaging period. We tracked the position of individual cells at each 2-min time interval and used these data to measure migration velocity and directionality (Fig. 6). Directionality was defined as the ratio of the actual distance moved to the shortest distance between start and end of migration. NCCs in *chokh;Tg(sox10:GFP)* embryos migrated at an average rate of  $0.68 \pm 0.17 \mu\text{m}/\text{min}$ , which was significantly slower than control rates of  $0.91 \pm 0.35 \mu\text{m}/\text{min}$  in *Tg(sox10:GFP)* embryos (Fig. 6C). Moreover, NCCs in *chokh* embryos displayed significantly less directed migration than controls (directionality ratios of 0.84 vs. 0.93, respectively), and instead wandered in multiple directions (Fig. 6B,C). Thus, even at stages before NCCs reach the normal eye vesicle location, their migration is defective in *chokh* embryos.

While much less affected, NCCs in the medial stream also do not behave normally in *chokh* embryos: they appear to enter their migratory route prematurely and do not migrate as fast as NCCs in WT embryos (Fig. 5B, arrow). Nevertheless, these cells migrate with the correct trajectory and eventually reach their target area.

Finally, we asked whether the defects in NCC migration in *chokh* mutants would translate into aberrant development of neural crest-derived

periocular tissues, such as orbital cartilages. Alcian blue staining of *chokh* mutant embryos showed mild defects in jaw cartilage development. All elements of the upper and lower jaw were present and at most slightly malformed (Fig. 7), which we attribute to mechanical deformation due to loss of the eye. In contrast, the neurocranium had more severe defects in *chokh* embryos, which exhibited a loss of most of the ethmoid plate and a minor shortening of the trabeculae (Fig. 7). This phenotype was somewhat variable, but a complete ethmoid plate was never present. Not surprisingly, the fine dorsal orbital cartilages (anterior and posterior orbital, epiphyseal) were also absent in *chokh* embryos (data not shown). We conclude that a normally developing eye is necessary for the development of some cranial cartilages, but dispensable for most.

## DISCUSSION

In this study, we show that NCCs from the mesencephalon and diencephalon populate the orbit, the frontal nasal process, and the eye itself. We also confirmed results obtained by others that these NCCs split into different migratory streams and that only posterior midbrain and midbrain–hindbrain boundary-derived NCCs contribute to the first branchial arch (Wada et al., 2005; Eberhart et al., 2006). Furthermore, we show that the eye plays a crucial role in guiding migration of NCCs. In eyeless *chokh* embryos, NCCs in the dorsal migratory stream fail to migrate anteriorly. Time-lapse analysis of cell behaviors

demonstrated that these cells have significantly reduced rate and directionality even before they reach the normal eye position, suggesting they require signals from the eye to initiate directed migration. The ultimate consequence of this migratory defect is the absence of the ethmoid plate and orbital cartilage elements later in development.

Soules and Link (2005) recently demonstrated that mesenchymal cells contribute to the anterior segment of the zebrafish eye, and that the development of the anterior segment is largely conserved between zebrafish and other vertebrates. Our fate mapping results show that NCCs from the mesencephalon and diencephalon contribute to the eye and orbit of the zebrafish. The fate map is remarkably similar to that obtained in the chick and mouse embryos (Le Douarin, 2004; Gage et al., 2005; Kanakubo et al., 2006), suggesting that zebrafish will be an excellent model organism for further study of these cells.

Previous research on mechanisms of cranial NCC migration has mostly focused on hindbrain-derived populations. Of interest, all guidance molecules identified in this context act by restricting or inhibiting cell migration. For example, ErbB4-mediated signaling helps to maintain an NCC exclusion zone in rhombomere three (Golding et al., 2000, 2002, 2004). Eph-ephrin signaling prevents intermingling of second and third branchial arch migration streams (Smith et al., 1997), while Semaphorin signaling creates NCC exclusion zones lateral to the hindbrain (Yu and Moens, 2005) and prevents intermingling of first

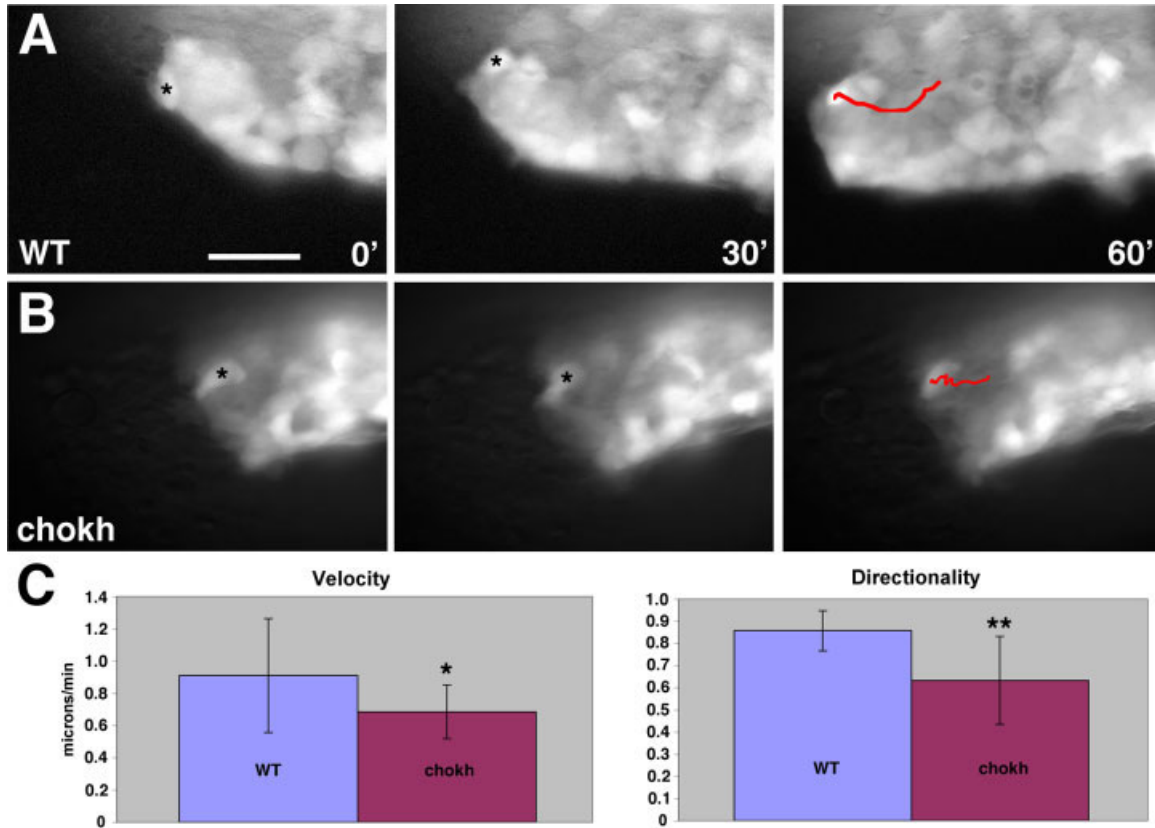


**Fig. 6.** Anterior neural crest cells (NCCs) have reduced migration rates and directionality in *chokh*. **A,B:** Stills from time-lapse movies at higher magnification of a wild-type (WT, A) and a *chokh* mutant embryo (B) in the *Tg(sox10:gfp)* background. Red lines in 60-min panels show the tracking position at each 2-min interval of the cells marked by asterisks in the 0-min and 30-min panels. **C:** Results of velocity and directionality measurements. Cells were tracked over 20 to 60 min. Values shown are the mean, and error bars are standard deviation.  $n = 21$  cells in 5 embryos for WT and 26 cells in 5 embryos for *chokh* embryos. Means were compared with unpaired *t*-tests. \* $P = 0.0061$ ; \*\* $P < 0.0001$ . Scale bar = 50  $\mu\text{m}$ .

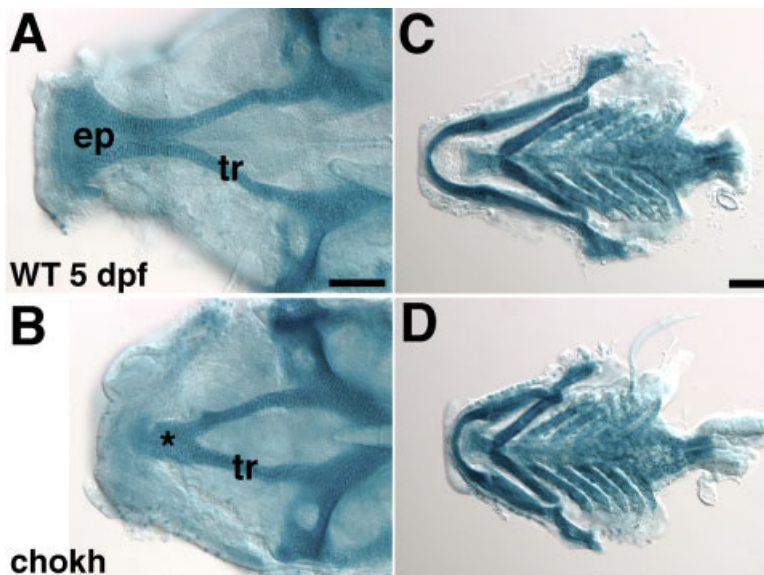


**Fig. 7.** Cranial cartilages are affected in *chokh* mutant embryos. **A–D:** Alcian blue stained wild-type (WT) and *chokh* mutant dissected neurocranium (A,B) and lower jaw (C,D) at 5 days postfertilization (dpf). Ventral views, anterior is to the left. Scale bars = 25  $\mu\text{m}$  in A,B, 100  $\mu\text{m}$  in C,D.

and second arch migration streams (Gammill et al., 2007). Our results showing failed migration of anterior NCCs in the absence of the eye provide the first demonstration that positive cues from target tissues are important for proper cranial NCC migration. Moreover, the fact that NCCs in the *chokh* mutant migrate slowly and with poor directionality even before reaching the normal position of the eye suggests that the eye potentially secretes a signal that attracts these cells from a distance. NCCs slightly more posterior, on the other hand, still migrate to their correct targets and are able to form the trabeculae in the ventral midline of the skull, arguing that their normal migratory environment is not altered in the absence of the eye. Little else is known about the migration of anterior NCCs. Two studies showed that a hedgehog signal is required for the condensation and differentiation of neurocranial NCCs at the zebrafish

midline (Wada et al., 2005; Eberhart et al., 2006), although this signal appears to be required after migration to the target region is largely complete. To our knowledge, no other positive or negative guidance cues for diencephalic and mesencephalic NCCs have been identified to this point.

The finding that anterior cranial NCCs require the presence of the eye to migrate correctly may have ramifications for research on craniofacial development. Craniofacial malformations account for the largest fraction of human birth defects, with approximately 30% falling into this category. It seems plausible that malformations of the ventral neurocranium may be traced back to abnormal expression levels of, for example, secreted signals from the eye or adhesion or extracellular matrix molecules along the dorsal surface of the budding eye vesicle. Further work will be necessary to elucidate the molecular nature of the guidance signals provided by the eye.

Other fundamental questions about anterior cranial NCC migration remain to be answered. For example, how are NCCs separated into different migratory streams? Is there any signal intrinsic to NCCs that prefigures them for one of the routes? And if not, do they pick one trajectory simply by their initial position along the anterior-posterior axis? As opposed to hindbrain NCCs, which form spatially separated streams, diencephalic and mesencephalic NCCs appear to form a much less ordered mass of cells dorsal and posterior to the eye. Yet, they come from an area of the brain that appears to be segmented like the hindbrain (Larsen et al., 2001; Zervas et al., 2004; Langenberg and Brand, 2005). It will be of interest to determine whether similar or novel signaling pathways and adhesion molecules influence the migration of NCCs to the eye and neurocranium.

## EXPERIMENTAL PROCEDURES

### Fish Maintenance

Wild-type (AB) and mutant *chokh* (*chk<sup>s399</sup>*) (Loosli et al., 2003) zebrafish (*Danio rerio*) embryos were obtained from natural group or pair-wise matings. For experiments in Figures 4, 5,

and 6, we used *Tg(sox10:gfp)* transgenic embryos (Wada et al., 2005). Embryos were reared at 23–29.5°C in E3 embryo medium and staged according to Kimmel et al. (1995). Hours or days postfertilization (hpf or dpf) were defined as time reared at 28.5°C.

### In Situ Hybridization

Single and two-color in situ hybridization was essentially carried out as described (Halloran et al., 1998). Digoxigenin- or fluorescein isothiocyanate (FITC)-labeled probes for the following genes were used: *snail2* (Thisse et al., 1995), *sox10* (Dutton et al., 2001), *crestin* (Luo et al., 2001), *six3* (Kobayashi et al., 1998), *six4a* (Seo et al., 1998), *pax6* (Krauss et al., 1991), and *fgf8* (Reifers et al., 1998).

### Cartilage Staining

Larvae were fixed in 4% paraformaldehyde at 5 dpf and stained for cartilage with Alcian blue as described (Schilling et al., 1996), except that embryos were not trypsinized.

### FITC-uncaging

One-cell stage embryos were injected with 1 nl of 2% DMNB-caged FITC-dextran ( $10 \times 10^3$  Mr, Molecular Probes, Eugene, OR). Embryos were dechorionated and oriented laterally in 4% methyl cellulose. The fluorophore was uncaged by means of illumination at 360 nm with a  $\times 60$  dipping objective. Exposure for 1 sec through a pinhole aperture was controlled by an automated shutter. Embryos were fixed 24 hr later. Uncaged FITC-dextran was detected by an antibody specific to FITC, conjugated to alkaline phosphatase (Roche; Keegan et al., 2004).

### Live Imaging

*Tg(sox10:gfp)* and *chokh;Tg(sox10:gfp)* embryos at the 8–10 ss were dechorionated and oriented laterally in 1.25% agarose in Danieau medium. Time-lapse acquisition was carried out on a Nikon E600 epifluorescent microscope equipped with a CoolSnap HQ CCD camera (Photometrics), automated filter wheel and microscope stage controlled by the Metamorph (Universal Imaging) software. For low-magnifica-

tion images, stacks were acquired every 5 min for up to 7 hr with 5  $\mu$ m z-spacing. For higher magnification cell tracking, stacks were acquired every 2 min over 1 hr with 2  $\mu$ m z-spacing. Stacks were flattened into single images using a maximum projection algorithm, and cells were tracked using Metamorph software.

## ACKNOWLEDGMENTS

We thank Dr. Tom Schilling for the *Tg(sox10:gfp)* transgenic line, Dr. Herwig Baier for the *chokh* mutant line, and Dr. Brian Link for helpful discussions. We also thank Drs. Jenya Grinblat, Michael Brand, Anders Fjose, and Hee-Chan Seo for cDNAs. A.K. was supported by an unrestricted grant from Research to Prevent Blindness to the Department of Ophthalmology and Visual Sciences at the University of Wisconsin. M.C.H. was funded by the NIH and T.L. was funded by a DFG fellowship.

## REFERENCES

- Chan WY, Tam PP. 1988. A morphological and experimental study of the mesencephalic neural crest cells in the mouse embryo using wheat germ agglutinin-gold conjugate as the cell marker. *Development* 102:427–442.
- Chuang JC, Mathers PH, Raymond PA. 1999. Expression of three Rx homeobox genes in embryonic and adult zebrafish. *Mech Dev* 84:195–198.
- Couly G, Le Douarin NM. 1990. Head morphogenesis in embryonic avian chimeras: evidence for a segmental pattern in the ectoderm corresponding to the neuromeres. *Development* 108:543–558.
- Couly GF, Coltey PM, Le DN. 1992. The developmental fate of the cephalic mesoderm in quail-chick chimeras. *Development* 114:1–15.
- Couly GF, Coltey PM, Le Douarin NM. 1993. The triple origin of skull in higher vertebrates: a study in quail-chick chimeras. *Development* 117:409–429.
- Couly GF, Le Douarin NM. 1987. Mapping of the early neural primordium in quail-chick chimeras. II. The prosencephalic neural plate and neural folds: implications for the genesis of cephalic human congenital abnormalities. *Dev Biol* 120:198–214.
- Creuzet S, Vincent C, Couly G. 2005. Neural crest derivatives in ocular and periorbital structures. *Int J Dev Biol* 49:161–171.
- Cubbage CC, Mabee PM. 1996. Development of the cranium and paired fins in the zebrafish *Danio rerio*. *J Morphol* 299:121–160.

- Cvekl A, Tamm ER. 2004. Anterior eye development and ocular mesenchyme: new insights from mouse models and human diseases. *Bioessays* 26:374–386.
- Dutton KA, Pauliny A, Lopes SS, Elworthy S, Carney TJ, Rauch J, Geisler R, Haffter P, Kelsh RN. 2001. Zebrafish colourless encodes *sox10* and specifies non-ectomesenchymal neural crest fates. *Development* 128:4113–4125.
- Eberhart JK, Swartz ME, Crump JG, Kimmel CB. 2006. Early Hedgehog signaling from neural to oral epithelium organizes anterior craniofacial development. *Development* 133:1069–1077.
- Gage PJ, Rhoades W, Prucka SK, Hjalt T. 2005. Fate maps of neural crest and mesoderm in the Mammalian eye. *Invest Ophthalmol Vis Sci* 46:4200–4208.
- Gammill LS, Gonzalez C, Bronner-Fraser M. 2007. Neuropilin 2/semaphorin 3F signaling is essential for cranial neural crest migration and trigeminal ganglion condensation. *Dev Neurobiol* 67:47–56.
- Golding JP, Trainor P, Krumlauf R, Gassmann M. 2000. Defects in pathfinding by cranial neural crest cells in mice lacking the neuregulin receptor ErbB4. *Nat Cell Biol* 2:103–109.
- Golding JP, Dixon M, Gassmann M. 2002. Cues from neuroepithelium and surface ectoderm maintain neural crest-free regions within cranial mesenchyme of the developing chick. *Development* 129:1095–1105.
- Golding JP, Sobieszczuk D, Dixon M, Coles E, Christiansen J, Wilkinson D, Gassmann M. 2004. Roles of *erbB4*, rhombomere-specific, and rhombomere-independent cues in maintaining neural crest-free zones in the embryonic head. *Dev Biol* 266:361–372.
- Halloran MC, Severance SM, Yee CS, Gemza DL, Kuwada JY. 1998. Molecular cloning and expression of two novel zebrafish semaphorins. *Mech Dev* 76:165–168.
- Jiang X, Iseki S, Maxson RE, Sucov HM, Morriss-Kay GM. 2002. Tissue origins and interactions in the mammalian skull vault. *Dev Biol* 241:106–116.
- Johnston MC, Noden DM, Hazelton RD, Coulombre JL, Coulombre AJ. 1979. Origins of avian ocular and periocular tissues. *Exp Eye Res* 29:27–43.
- Kanakubo S, Nomura T, Yamamura K, Miyazaki J, Tamai M, Osumi N. 2006. Abnormal migration and distribution of neural crest cells in *Pax6* heterozygous mutant eye, a model for human eye diseases. *Genes Cells* 11:919–933.
- Keegan BR, Meyer D, Yelon D. 2004. Organization of cardiac chamber progenitors in the zebrafish blastula. *Development* 131:3081–3091.
- Kennedy BN, Stearns GW, Smyth VA, Ramamurthy V, van Eeden F, Ankoudinova I, Raible D, Hurley JB, Brockerhoff SE. 2004. Zebrafish *rx3* and *mab2112* are required during eye morphogenesis. *Dev Biol* 270:336–349.
- Kimmel CB, Ballard WW, Kimmel SR, Ullmann B, Schilling TF. 1995. Stages of embryonic development of the zebrafish. *Dev Dyn* 203:253–310.
- Kobayashi M, Toyama R, Takeda H, Dawid IB, Kawakami K. 1998. Overexpression of the forebrain-specific homeobox gene *six3* induces rostral forebrain enlargement in zebrafish. *Development* 125:2973–2982.
- Krauss S, Johansen T, Korzh V, Moens U, Ericson JU, Fjose A. 1991. Zebrafish *pax[zf-a]*: a paired box-containing gene expressed in the neural tube. *EMBO J* 10:3609–3619.
- Langenberg T, Brand M. 2005. Lineage restriction maintains a stable organizer cell population at the zebrafish midbrain-hindbrain boundary. *Development* 132:3209–3216.
- Larsen CW, Zeltser LM, Lumsden A. 2001. Boundary formation and compartment in the avian diencephalon. *J Neurosci* 21:4699–4711.
- Le Douarin NM. 2004. The avian embryo as a model to study the development of the neural crest: a long and still ongoing story. *Mech Dev* 121:1089–1102.
- Le Lievre CS. 1978. Participation of neural crest-derived cells in the genesis of the skull in birds. *J Embryol Exp Morphol* 47:17–37.
- Loosli F, Staub W, Finger-Baier KC, Ober EA, Verkade H, Wittbrodt J, Baier H. 2003. Loss of eyes in zebrafish caused by mutation of *chokh/rx3*. *EMBO Rep* 4:894–899.
- Luo R, An M, Arduini BL, Henion PD. 2001. Specific pan-neural crest expression of zebrafish *Crestin* throughout embryonic development. *Dev Dyn* 220:169–174.
- Meier S. 1982. The distribution of cranial neural crest cells during ocular morphogenesis. *Prog Clin Biol Res* 82:1–15.
- Noden DM. 1975. An analysis of migratory behavior of avian cephalic neural crest cells. *Dev Biol* 42:106–130.
- Noden DM. 1983. The embryonic origins of avian cephalic and cervical muscles and associated connective tissues. *Am J Anat* 168:257–276.
- Noden DM. 1986a. Origins and patterning of craniofacial mesenchymal tissues. *J Craniofac Genet Dev Biol Suppl* 2:15–31.
- Noden DM. 1986b. Patterning of avian craniofacial muscles. *Dev Biol* 116:347–356.
- Osumi-Yamashita N, Ninomiya Y, Doi H, Eto K. 1994. The contribution of both forebrain and midbrain crest cells to the mesenchyme in the frontonasal mass of mouse embryos. *Dev Biol* 164:409–419.
- Reifers F, Böhlh H, Walsh EC, Crossley PH, Stainier DYR, Brand M. 1998. *Fgf8* is mutated in zebrafish acerebellar mutants and is required for maintenance of midbrain-hindbrain boundary development and somitogenesis. *Development* 125:2381–2395.
- Rojas-Munoz A, Dahm R, Nusslein-Volhard C. 2005. *chokh/rx3* specifies the retinal pigment epithelium fate independently of eye morphogenesis. *Dev Biol* 288:348–362.
- Schilling TF, Kimmel CB. 1994. Segment and cell type lineage restrictions during pharyngeal arch development in the zebrafish embryo. *Development* 120:483–494.
- Schilling TF, Piotrowski T, Grandel H, Brand M, Heisenberg C-P, Jiang Y-J, Beuchle D, Hammerschmidt M, Kane DA, Mullins MC, van Eeden FJM, Kelsh RN, Furutani-Seiki M, Granato M, Haffter P, Odenthal J, Warga RM, Nusslein-Volhard C. 1996. Jaw and branchial arch mutants in zebrafish I: branchial arches. *Development* 123:329–344.
- Seo HC, Drivenes O, Fjose A. 1998. A zebrafish *Six4* homologue with early expression in head mesoderm. *Biochim Biophys Acta* 1442:427–431.
- Serbedzija GN, Bronner-Fraser M, Fraser SE. 1992. Vital dye analysis of cranial neural crest cell migration in the mouse embryo. *Development* 116:297–307.
- Smith A, Robinson V, Patel K, Wilkinson DG. 1997. The *EphA4* and *EphB1* receptor tyrosine kinases and ephrin-B2 ligand regulate targeted migration of branchial neural crest cells. *Curr Biol* 7:561–570.
- Soules KA, Link BA. 2005. Morphogenesis of the anterior segment in the zebrafish eye. *BMC Dev Biol* 5:12.
- Stigloher C, Ninkovic J, Laplante M, Geling A, Tannhauser B, Topp S, Kikuta H, Becker TS, Houart C, Bally-Cuif L. 2006. Segregation of telencephalic and eye-field identities inside the zebrafish forebrain territory is controlled by *Rx3*. *Development* 133:2925–2935.
- Thisse C, Thisse B, Postlethwait JH. 1995. Expression of *snail2*, a second member of the zebrafish *snail* family, in cephalic mesoderm and presumptive neural crest of wild-type and spadetail mutant embryos. *Dev Biol* 172:86–99.
- Trainor PA, Tam PP. 1995. Cranial paraxial mesoderm and neural crest cells of the mouse embryo: co-distribution in the craniofacial mesenchyme but distinct segregation in branchial arches. *Development* 121:2569–2582.
- Trainor PA, Tan SS, Tam PP. 1994. Cranial paraxial mesoderm: regionalisation of cell fate and impact on craniofacial development in mouse embryos. *Development* 120:2397–2408.
- Wada N, Javidan Y, Nelson S, Carney TJ, Kelsh RN, Schilling TF. 2005. Hedgehog signaling zebrafish skull. *Development* 132:3977–3988.
- Yu HH, Moens CB. 2005. Semaphorin signaling guides cranial neural crest cell migration in zebrafish. *Dev Biol* 280:373–385.
- Zervas M, Millet S, Ahn S, Joyner AL. 2004. Cell behaviors and genetic lineages of the mesencephalon and rhombomere 1. *Neuron* 43:345–357.